

# New mechanism of formation of discrete luminescence spectra of excitons localized at point defect clusters

V. F. Agekyan, L. G. Gerchikov, and V. A. Kharchenko

*A. A. Zhdanov State University, Leningrad*

(Submitted 14 July 1986)

*Zh. Eksp. Teor. Fiz.* **92**, 1770–1781 (May 1987)

Experimental and theoretical investigations were made of a new type of discrete exciton-impurity luminescence spectra. The existence of a discrete series of lines converging in the low-frequency part of the spectrum was attributed to selective population of exciton states localized at groups (clusters) of point defects. The population selectivity appears because of resonance capture of excitons by clusters with specific geometric configurations. The model of a zero-radius potential is used to calculate the energy spectrum of resonance clusters and a good agreement with the experimentally recorded spectra is obtained in the case of tin dioxide crystals. The resonance cross sections for the capture of excitons by clusters are calculated. The physical and geometric parameters of clusters consisting of two, three, or four oxygen vacancies are determined for an SnO<sub>2</sub> crystal. It is shown that disappearance of the discrete structure of the luminescence spectra of excitons localized at clusters on increase in temperature, pumping rate, or defect concentration is due to suppression of the resonance capture mechanism.

A large proportion of recent investigations of the exciton-impurity luminescence of semiconductor crystals is devoted to excitons localized at groups of point defects. A general analysis of the experimental results<sup>1-7</sup> makes it possible to identify two types of discrete luminescence spectra in the form of series of lines converging either in the high-frequency part of the spectrum or at the low-frequency end. The first type corresponds to the recombination of Mott excitons localized at pair defects with a pair radius varying in discrete steps,<sup>1-4</sup> already thoroughly investigated and outside the scope of the present paper. Spectra of the second type, recently observed experimentally,<sup>5-7</sup> are due to radiative recombination of excitons localized at groups (clusters) of closely spaced defects. The average distance between the defects in such clusters is usually considerably greater than the radius of the potentials created by point defects. For each value of the energy in the discrete exciton-impurity luminescence spectrum there is an exciton state localized at a cluster with a specific number of defects. Even clusters consisting of the same numbers of defects can have different geometric configurations, and, therefore, different energies of their localized exciton states. This would seem to exclude the possibility of observation of discrete lines in the luminescence spectra. We shall show that the reason for the formation of the discrete spectra of excitons bound to clusters is the resonance nature of the capture of excitons by clusters with distinctly defined geometric configurations. Such clusters create excited energy levels near the boundary of the continuous exciton spectrum. These excited levels are manifested directly in the exciton luminescence spectra and they increase strongly the probability of exciton capture by the appropriate clusters. Therefore, resonance clusters are populated more effectively than the others and, consequently, they are the ones that are manifested first in the exciton luminescence spectra. We shall provide a qualitative description of the mechanism of resonance capture by using as an example the

simplest cluster consisting of two point defects. An exciton localized by such a pair of defects may be in two states: ground and excited (antibonding). The luminescence process corresponds to the ground state, which determines the energy of the emitted photons. Since the distance between defects in pairs can have various values, the energy of the ground state of excitons localized at these pairs may vary within fairly wide limits. There are pairs with the excited state energy close to the limit of the continuous spectrum of excitons. The distance between defects in such pairs is fixed and, therefore, the ground state energy is fixed. These are the pairs that effectively capture free excitons: the presence of an antibonding state close to the limit of the continuous spectrum causes resonance scattering of free excitons, which in turn increases by several orders of magnitude the capture cross section of the ground state. We can say that out of all the pairs with different radii only the resonance pairs are populated effectively and the luminescence spectra should exhibit peaks corresponding solely to such pairs with a definite value of the localized exciton energy. Discrete lines in the luminescence spectra of excitons localized at clusters consisting of three, four, or more point defects appear in a similar manner. Selective population of clusters with resonance properties is responsible for the discrete structure of the luminescence spectra of localized excitons. We shall report experimental and theoretical investigations of the cases when suppression by some method or another (for example, by an increase in temperature or the concentration of defects) of the resonance scattering destroys the discrete structure in the exciton-impurity luminescence spectra.

It follows from this qualitative discussion that we are dealing with a new mechanism of formation of discrete exciton-impurity luminescence spectra when the discrete structure is not due to specific behavior of the density of states, but due to selectivity of filling the energy levels corresponding to excitons localized at clusters with resonance configura-

rations. A study of this mechanism is important in the case of solid solutions of semiconductor compounds and of crystals with high concentrations of intrinsic defects, particularly if there is a tendency for the defects to form clusters under certain external perturbations.<sup>8</sup>

The theoretical model proposed in the present paper explains well the principal properties of the luminescence spectra of excitons localized at clusters of point defects: the energy positions of the lines, and the dependences of the spectra on the defect concentration and temperature. In an analysis of the experimental results the main attention will be paid to the luminescence spectra of excitons localized at clusters of oxygen vacancies in tin dioxide crystals. A well-resolved discrete structure of these spectra investigated at various temperatures and for different defect concentrations made it possible to determine from the experimental data the physical and geometric characteristics of "resonance" clusters.

### 1. ABSORPTION AND LUMINESCENCE SPECTRA OF TIN DIOXIDE

We investigated in detail the absorption luminescence spectra of excitons bound to single oxygen vacancies and to groups of such vacancies in SnO<sub>2</sub>. Tin dioxide is a tetragonal crystal belonging to the rutile group with the  $D_{4h}^{14}$  symmetry in a unit cell of  $0.5 \times 0.5 \times 0.3$  nm dimensions containing four oxygen atoms and two atoms of tin. Spectroscopic investigations of crystals of this group have been seriously delayed by the poor quality of the crystals, but the development of new growth methods, particularly high-temperature synthesis of SnO<sub>2</sub> from SnCl<sub>4</sub> and H<sub>2</sub>O vapor, has made it possible to prepare crystals with easily resolved exciton spectra. The lattices of GeO<sub>2</sub>, SnO<sub>2</sub>, and TiO<sub>2</sub> are known to exhibit a tendency to form oxygen vacancies and, depending on the annealing conditions (temperature, oxygen pressure), the concentration of these vacancies can be varied within a wide range and changes in the concentration are largely reversible. This property, used in some technical applications, makes SnO<sub>2</sub> a convenient model object for the investigation of intrinsic defects in a crystal.

**Absorption spectrum.** The short-wavelength absorption edge of SnO<sub>2</sub> is polarized parallel to the c tetragonal axis and is structure-free. The long-wavelength edge is polarized perpendicular to the c axis and it corresponds to a direct forbidden transition  $\Gamma_3^+ \rightarrow \Gamma_1^+$  with a band gap of 3.596 eV at  $T = 2$  K; a series of narrow exciton lines converges at this edge<sup>9,10</sup> (Fig. 1a). In the case of dipole lines with the quantum numbers  $n = 2, 3, \dots, 6$  (exciton symmetry  $P_{\pm 1}$ ) the condition of hydrogen-like behavior with an effective Rydberg constant  $R_{\pm 1} = 0.0322$  eV is satisfied exactly. In a magnetic field another series with  $R_0 = 0.0275$  eV becomes dipole-allowed (exciton symmetry  $P_0$ ) and it converges at the same limit. The published values of  $R_{\pm 1}$  and  $R_0$  (Ref. 11) and the effective masses of an electron  $m_e^{\parallel} = 0.275m_0$  and  $m_e^{\perp} = 0.299m_0$ , deduced from the cyclotron resonance experiments,<sup>12</sup> can be used to estimate the effective mass of a hole  $m_h \approx 5m_0$ , i.e., in the case of SnO<sub>2</sub> we have  $m_e \ll m_h$ .

The absorption spectra of SnO<sub>2</sub> crystals with different concentrations of oxygen vacancies  $n_0$  are plotted in Fig. 1. Lines corresponding to the ground  $E_1'$  and excited ( $1'-5'$ ) states of the internal motion of an exciton localized at a sin-

gle oxygen vacancy appear and become stronger as  $n_0$  is increased; in this case an exciton is in a state  $n \geq 2$ . This is followed by splitting of the spectrum of a free exciton and at high concentrations  $n_0$  the discrete exciton absorption lines are converted into a step which extends toward longer wavelengths.<sup>13</sup> This form of the spectrum corresponds to delocalization of electrons bound to oxygen impurities and then the states with finite momenta may appear in zero-phonon exciton spectra because of breakdown of the selection rules. An estimate of the vacancy concentration for samples with similar intensities of the  $E_1$  and 1S absorption lines of free excitons (Fig. 1b) gives  $n_0 \sim 10^{17}$  cm<sup>-3</sup>. If the splitting of the 1S absorption lines of free excitons occurs at such oxygen vacancy concentrations that the distance between these vacancies becomes of the order of the Bohr radius of a free exciton, we find that the spectra in Figs. 1c and 1d correspond to vacancy concentrations  $n_0 \approx 10^{18}$  cm<sup>-3</sup> and  $n_0 = 10^{19}$  cm<sup>-3</sup>.

**Luminescence spectra.** The exciton luminescence of SnO<sub>2</sub> at  $T = 2$  K consists of zero-phonon recombination lines of bound and free excitons and their phonon replicas; we shall analyze only the zero-phonon part of the spectrum. The spectrum of bound excitons of interest to us consists of five  $E_1-E_5$  lines converging on the long-wavelength side (Fig. 1a') and the  $E_1$  line is in resonance with the absorption line. The spectrum in Fig. 1a' represents a crystal in which oxygen vacancies were not deliberately introduced and were not manifested in the absorption spectrum. An increase in  $n_0$  weakens the free-exciton luminescence and the intensity of the bound-exciton luminescence becomes redistributed in favor of long-wavelength lines (Figs. 1b' and 1c'). The lines  $E_1-E_5$  should be attributed to excitons bound to clusters consisting of  $N$  closely spaced oxygen vacancies, where  $N = 1, 2, 3, \dots$

**Temperature dependence of the luminescence.** Heating from  $T = 2$  K weakens monotonically the 1S free-exciton luminescence line, so that it can be observed only up to 30 K whereas the line  $E_1$  becomes stronger in the interval 2–20 K (Fig. 2). The lines  $E_2-E_5$  become weaker on increase in temperature, so that the strongest line in the spectra of all the

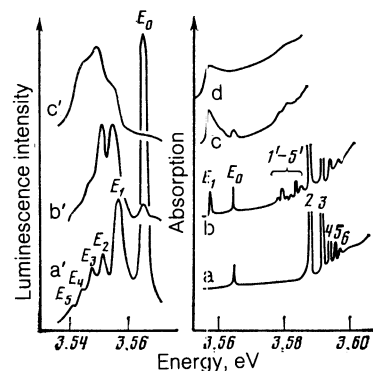


FIG. 1. Exciton spectra of SnO<sub>2</sub> recorded at  $T = 2$  K (zero-phonon region). The absorption spectra are shown on the right;  $E_0$  is the 1S state of a free exciton, whereas lines 2, 3, 4, 5, and 6 correspond to the quantum numbers  $n = 2, 3, 4, 5, 6$ ;  $E_1$  and  $1'-5'$  are the ground excited states of a complex formed from an exciton and a single oxygen vacancy. The concentration of oxygen vacancies increases from a to d. The luminescence spectra are on the left. The lines  $E_N$  ( $N = 1, 2, \dots, 5$ ) represent excitons localized at clusters consisting of  $N$  oxygen vacancies. The absorption spectra a, b, and c correspond to the luminescence spectra a', b', c'.

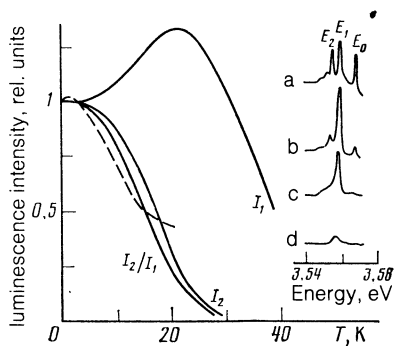


FIG. 2. Temperature dependences of the normalized intensities  $I_1$  and  $I_2$  of the luminescence lines  $E_1$  and  $E_2$  and of their ratio  $I_2/I_1$ . The dashed curve is calculated on the basis of Eq. (13) assuming that  $\varepsilon_2^- = 1$  meV and  $s = 4 \times 10^5$  cm/sec. The exciton luminescence spectrum of  $\text{SnO}_2$  recorded at  $T = 2$  K (a), 20 K (b), 30 K (c), and 50 K (d) is shown on the right.

crystals at  $T = 20$  K is  $E_1$  irrespective of the initial distribution of the intensity. The temperature dependences of the  $E_1$  and free-exciton lines are unusual because in most cases the free-exciton luminescence line is enhanced by an increase in temperature due to the activation of excitons localized at defects. The disappearance of the free-exciton luminescence line at  $T = 30$  K and the considerable brightness of the  $E_1$  line of localized excitons at the same temperature are evidence of the existence of nonradiative exciton recombination centers. An increase in the mobility of free excitons on increase in  $T$  should result in faster loss of these excitons at such centers.

**Charge state of defects.** An investigation of the luminescence of  $\text{SnO}_2$  crystals with low concentrations of vacancy clusters carried out at different pulse excitation rates  $J$  demonstrated (Fig. 3) that at relatively low rates of excitation it is the free-exciton luminescence that predominates, but in the case of strong excitation the relative contribution of the lines  $E_1$ - $E_5$  becomes stronger. The dependence of the intensity of the free-exciton luminescence on  $J$  is slightly sublinear, whereas the growth of the bound-exciton luminescence is superlinear. The superlinearity can be explained by an increase in the concentration of the centers at which excitons are localized: as  $J$  is increased, an increasing proportion of the initially charged oxygen vacancies becomes neutral. Therefore, lines due to excitons localized at neutral oxygen vacancies appear in the spectrum of  $\text{SnO}_2$ . It should be pointed out that at the maximum values of  $J$  used in our study the line  $E_1$  is enhanced in the spectrum  $E_1$ - $E_5$  and the discrete structure of the other line becomes smeared out. We shall show below that this is due to a decreasing role of the resonance capture of excitons by oxygen vacancy clusters because of the high concentration of free excitons.

## 2. THEORETICAL ANALYSIS OF EXCITON LUMINESCENCE SPECTRA OF $\text{SnO}_2$

We shall now consider a theoretical model which can account for all the experimentally observed properties of the exciton luminescence spectrum of tin dioxide: the existence of a discrete series of luminescence lines  $E_1$ - $E_5$  converging in the long-wavelength part of the spectrum; the ratios of the intensities of the lines  $E_1$ - $E_5$  at various temperatures; the nonmonotonic temperature dependence of the intensity of

the line  $E_1$  (Fig. 2); the dependence of the luminescence spectrum on the concentration of oxygen vacancies.

We must point out first that the binding energy<sup>1)</sup> of excitons at isolated vacancies  $\varepsilon_1 \approx -8$  meV is considerably less than the binding energy of internal motion of an exciton (Rydberg constant). We can therefore use the well-known model of Rashba<sup>14</sup> for weakly bound excitons. The use of this model in our case means that a neutral oxygen vacancy creates a short-range potential which localizes the motion of the center of mass of an exciton. In view of the large effective mass of a hole ( $m_e/m_h \ll 1$ ), the coordinate of the center of mass  $\mathbf{r}$  of an exciton eventually coincides with the coordinate of a hole so that when we speak of the motion of the whole exciton we need consider only the motion of a hole. The short-range potential created by a neutral oxygen vacancy is described in the model of a zero-radius potential by a single parameter which is the scattering length  $f$ . The binding energy  $\varepsilon_1$  and the wave function  $\Psi(\mathbf{r})$  of the center of mass of an exciton localized at an isolated oxygen vacancy are

$$\varepsilon_1 = -\frac{\hbar^2}{2m_h f^2}, \quad \Psi_1(\mathbf{r}) = \frac{\exp[-r/f]}{(2\pi f)^{3/2}}. \quad (1)$$

The experimental value of the binding energy  $\varepsilon_1$  makes it possible to estimate the absolute value of the scattering length, which is  $f = 0.9$  nm. Such a low value in the case of exciton processes is due to a large effective mass of a hole.

We shall now describe the motion of the center of mass of an exciton localized at a cluster consisting of  $N$  oxygen vacancies. The wave function of this exciton for the selected system of zero-radius potentials is<sup>15</sup>

$$\Psi(\mathbf{r}) = \sum_{i=1}^N C_i \frac{\exp[-\kappa|\mathbf{r}-\mathbf{R}_i|]}{|\mathbf{r}-\mathbf{R}_i|}, \quad \kappa = \left[ \frac{2m_h}{\hbar^2} |\varepsilon_N| \right]^{1/2}, \quad (2)$$

where  $\mathbf{R}_i$  are the radius vectors of oxygen vacancies in a cluster and  $C_i$  are the amplitude coefficients.

The wave function  $\Psi(\mathbf{r})$  is the exact solution for the model of zero-radius potentials and  $C_i$  is found by solving the secular equation

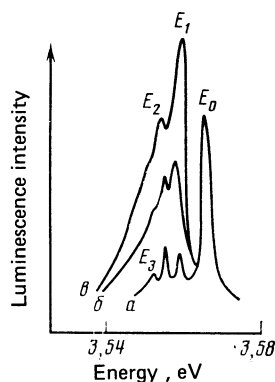


FIG. 3. Exciton luminescence of  $\text{SnO}_2$  normalized to the intensity of the free-exciton line  $E_0$  obtained at pulsed excitation rates of 20, 50, and 200  $\text{kW}/\text{cm}^2$  (a, b, and c, respectively).

$$C_i \left[ 1 - \left( \frac{\varepsilon_N}{\varepsilon_1} \right)^{1/2} \right] + \sum_{j=1}^N C_j \frac{\exp[-(\varepsilon_N/\varepsilon_1)^{1/2} R_{ij}/f]}{R_{ij}/f} = 0, \quad (3)$$

where  $R_{ij} = |\mathbf{R}_i - \mathbf{R}_j|$ . The binding energy  $\varepsilon_N$  is found by equating to zero the determinant of the system (3). The value of  $\varepsilon_N$  depends not only on the number of oxygen vacancies in a cluster, but is also greatly affected by the geometric characteristics of the cluster. It follows from Eq. (3) that variation over distances  $R_{ij}$  between oxygen vacancies in a cluster, expressed in units of the scattering length  $f$ , makes it possible to obtain the energy  $\varepsilon_N$  in units of  $\varepsilon_1$ . Therefore, there is no need to know the absolute value of  $f$  because only  $R_{ij}/f$  is important.

The simplest cluster consists of two oxygen vacancies separated by a distance  $R$ . In this case the equation for the binding energy of the center of mass of an exciton is

$$1 - (\varepsilon_2^\pm/\varepsilon_1)^{1/2} \pm (f/R) \exp[-(\varepsilon_2^\pm/\varepsilon_1)^{1/2} R/f] = 0. \quad (4)$$

The dependences of the energies of the excited  $\varepsilon_2^-$  and ground  $\varepsilon_2^+$  states of an exciton localized at a pair of oxygen vacancies on the distance  $R$  between them, obtained by solving Eq. (4), are plotted in Fig. 4. It should be noted that for  $R = f$  the energy of the excited state  $\varepsilon_2^-$  crosses the boundary of the continuous spectrum of an exciton (bottom of the exciton energy band). We shall show below that pairs of oxygen vacancies with such a radius have large resonance electron-capture cross sections, so that in the case of the pairs of oxygen vacancies manifested in the experimental luminescence spectra the relationship  $R \approx f$  should be obeyed. In fact, the energy position of the line  $E_2$  in the luminescence spectrum of  $\text{SnO}_2$  (Fig. 2) makes it possible to determine the binding energy of the center of mass of an exciton as  $\varepsilon_2^+ \approx -12$  meV and to find the radius of the corresponding oxygen vacancy pair  $R/f = 1 \pm 0.1$ . The error indicated for this quantity is governed by the experimental inaccuracies and the approximations of the theoretical model, which ignores the distortion of the internal motion of an exciton localized at an oxygen vacancy. In the region of  $R \approx f$  the error in the determination of the position  $\varepsilon_2^-$  from the experimental data is of the same order of magnitude as the value of  $\varepsilon_2^-$ , so that we may conclude that the energy of the excited state of a pair is close to the limit of the continuous spectrum:  $|\varepsilon_2^-| \lesssim 2$  meV. The permissible range of variation of  $R$  and  $f$ , subject to their errors, is represented by a rectangle in Fig. 4.

We shall now consider clusters with  $N = 3, 4, \dots$ . According to Eq. (3) this energy of the center of mass of an exciton localized at a cluster with a fixed value of  $N$  (there are always  $N$  levels, some of which may be in the continuous spectrum) depends on the geometric shape of a cluster and we have to find the large range of energies of the ground state  $\varepsilon_N$ . We might expect the appearance of numerous luminescence lines, but we shall show below that, out of the great variety of different clusters with  $N = 2, 3, 4, \dots$ , only those are manifested in the exciton luminescence spectra for which the exciton-capture cross section is anomalously large compared with the cross section for the capture by an isolated oxygen vacancy (it follows from the absorption spectra in Fig. 1 that the concentration of isolated oxygen vacancies is

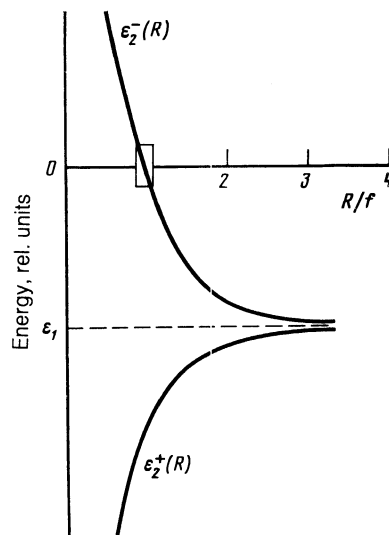


FIG. 4. Dependences of the energies of the ground and excited states  $\varepsilon_2^+$  and  $\varepsilon_2^-$  of the center of mass of an exciton localized at a pair of oxygen vacancies on the distance  $R$  between vacancies;  $f$  is the scattering length.

considerably higher than the concentration of vacancy clusters). Therefore, the large capture cross sections are exhibited by the clusters which have excited levels close to the bottom of the exciton energy band. In the case of clusters with the configurations of a regular triangle of side  $f$  ( $N = 3$ ) and a rhomb with a diagonal and sides  $f$  ( $N = 4$ ) a calculation carried out without specifying any parameters gives the ratio of the binding energies  $\varepsilon_4:\varepsilon_3:\varepsilon_2 = 1.48:1.31:1$ , which is in good agreement with the experimental results that yield 1.5:1.3:1 (lines  $E_4$ ,  $E_3$ , and  $E_2$ , respectively in Fig. 1). The same cluster configurations create resonance excited states with  $|\varepsilon| \lesssim 2$  meV. It would seem that for a given value of  $N$  there are numerous geometrically similar configurations of clusters with close values of the energies of exciton levels. However, in view of the discrete nature of the crystal lattice, a set of possible geometric configurations is also discrete. Since the distance between the vacancies in a cluster is of the order of several lattice constants, this discreteness results in a considerable difference between the binding energies  $\varepsilon_N$  of excitons even in the case of clusters with similar configurations. This is particularly important in the case of excited resonance energy levels, i.e., of the exciton capture cross sections.

A characteristic feature of the energy spectrum of excitons localized at oxygen vacancy clusters is the convergence of the series to large (in the absolute sense) values of the binding energy (convergence of the luminescence spectrum is in the direction of short wavelengths). This can be expected on the basis of the adopted model because as  $N$  increases the addition of a single oxygen vacancy to a cluster should have less and less effect on  $\varepsilon_N$ . In the limit of an infinite cluster of oxygen vacancies in  $\text{SnO}_2$  an exciton-impurity energy band is formed (more exactly, a band of exciton states which are initially localized at isolated oxygen vacancies) and the energy position of this band is estimated to be  $\varepsilon_\infty = -25$  meV. The value of  $\varepsilon_\infty$  is the limit at which the series of exciton lines localized as clusters converges. It should be stressed that convergence of the luminescence spectrum in Fig. 1a toward lower frequencies cannot be ex-

plained by the model of an exciton localized at a pair of defects with a discretely varying radius  $R$ : in this case there should be a reduction in the spacing between the lines at the short-wavelength end.

### 3. RESONANCE CAPTURE OF EXCITONS BY OXYGEN VACANCY CLUSTERS

We shall first consider the mechanism of resonance capture of excitons by clusters and the associated dependences of the luminescence spectrum on temperature and oxygen vacancy concentration. The following points should be borne in mind:

1) the probabilities of radiative recombination  $P$  of localized excitons corresponding to the spectral lines  $E_1$ - $E_5$  are close to one another and a rigorous calculation gives:  $P_1:P_2:P_3:P_4 = 1:0.87:0.82:0.84$ ;

2) when the concentration of oxygen vacancies becomes  $n_0 \sim 10^{17} \text{ cm}^{-3}$  (Fig. 1), the distance between isolated vacancies and particularly between vacancy clusters is an order of magnitude greater than the scattering length  $f$ .

This means that we can ignore migration of excitons between defects so that the relative intensities of the luminescence lines  $I_N$  are governed by the cluster concentrations  $n_N$  and by the exciton-capture cross sections of these clusters  $\sigma_N$ .

We shall consider the process of capture of excitons by isolated vacancy clusters and by pairs of clusters with a radius  $R$ . Using the example of pairs we shall demonstrate the role of a resonance process of capture in the formation of the luminescence spectra. In the range of temperatures  $T < 30 \text{ K}$  of interest to us the capture of excitons by isolated vacancy clusters is accompanied by the emission of acoustic phonons of energies  $|\varepsilon_N| \gg T$  and is a strongly inelastic process. Using the standard theory of the electron-phonon interaction, we shall obtain the cross section  $\sigma_N$  for the capture of a free exciton with a momentum  $\mathbf{k}$  by a cluster consisting of  $N$  vacancies:

$$\sigma_N = \frac{1}{2\pi} \left( \frac{w^2}{\hbar \rho s^2} \right) \left( \frac{m_h}{\hbar k} \right) q^3 \left\langle \left| \int \Psi_N^*(\mathbf{r}) e^{i\mathbf{q}\cdot\mathbf{r}} \Psi_i(\mathbf{r}) d^3r \right|^2 \right\rangle, \quad (5)$$

where  $w$  is the deformation potential constant;  $\rho$  is the density of the crystal;  $s$  is the velocity of sound;  $\Psi_i$  is the wave function of a free exciton which allows for its elastic scattering by a cluster of oxygen vacancies;  $\Psi_N$  is the wave function of the ground state of an exciton localized at a cluster of  $N$  vacancies ( $N = 1, 2, 3, \dots$ ). The angular brackets in Eq. (9) denote averaging over the angular variables of the quasimomentum of the emitted phonon  $|\mathbf{q}| = |\varepsilon_N|/\hbar s$  and of a free exciton  $\mathbf{k}$  (for a pair of oxygen vacancies this means averaging over all the angles of orientation of both  $\mathbf{k}$  and of the radius vector of a pair  $\mathbf{R}$ ). Since the quasimomentum of the emitted photons  $q$  is considerably greater than  $k$  and typical values of the momenta of bound states are of the order of  $(2m_h |\varepsilon_N|/\hbar^2)^{1/2} < q$ , an allowance for the scattered wave in  $\Psi_i$  during calculation of a matrix element in Eq. (5) is important even when the capture cross section  $\sigma_i$  of an isolated vacancy is determined:

$$\sigma_i = \frac{2w^2}{\hbar \rho s^3} \text{arctg}^2 \left[ \left( \frac{|\varepsilon_1|}{2m_h s^2} \right)^{1/2} \right] \left( \frac{|\varepsilon_1|}{\varepsilon} \right)^{1/2}, \quad (6)$$

where  $\varepsilon$  is the energy of a free exciton and  $\text{arctg}[(|\varepsilon_1|/2m_h s^2)^{1/2}] \approx \pi/2$ .

Equation (6) is a specific manifestation of the  $1/v$  law; at low velocities  $v$  the cross sections of the inelastic processes are inversely proportional to the particle velocity.<sup>16</sup> Clearly, Eq. (6) is valid for neutral vacancies creating a short-range potential.

We shall now calculate the capture cross section  $\sigma_2$  of a pair of oxygen vacancies with the coordinates of the vacancies  $\pm \mathbf{R}/2$ . The exact wave function allowing for the scattering of an exciton by this pair is

$$\Psi_i = e^{i\mathbf{k}\cdot\mathbf{r}} + f_+ \left\{ \frac{\exp[i\mathbf{k}\cdot(\mathbf{r}+\mathbf{R}/2)]}{|\mathbf{r}+\mathbf{R}/2|} + \frac{\exp[i\mathbf{k}\cdot(\mathbf{r}-\mathbf{R}/2)]}{|\mathbf{r}-\mathbf{R}/2|} \right\} + f_- \left\{ \frac{\exp[i\mathbf{k}\cdot(\mathbf{r}-\mathbf{R}/2)]}{|\mathbf{r}-\mathbf{R}/2|} - \frac{\exp[i\mathbf{k}\cdot(\mathbf{r}+\mathbf{R}/2)]}{|\mathbf{r}+\mathbf{R}/2|} \right\}, \quad (7)$$

where

$$f_+ = -\frac{\cos(\mathbf{k}\mathbf{R}/2)}{ik + f^{-1} + R^{-1} \exp(ikR)},$$

$$f_- = -\frac{i \sin(\mathbf{k}\mathbf{R}/2)}{ik + f^{-1} - R^{-1} \exp(ikR)}. \quad (8)$$

If  $R \approx f$ , when the excited-state energy  $\varepsilon_2^-$  lies close to the limit of the continuous spectrum of excitons, elastic scattering of excitons is of resonance nature, which follows from an analysis of the poles of  $f_-$  in Eq. (8). If we assume the specific value  $\varepsilon_2^- > 0$  (i.e.,  $R \lesssim f$ ), we can write down the resonance part of the amplitude  $g$  of elastic scattering in the standard form for  $kR \ll 1$ :

$$g_-(\theta') = -f_- \cdot 2i \sin \frac{\mathbf{k}'\mathbf{R}}{2}$$

$$= -\frac{2l+1}{2k} \frac{1/2 \Gamma \cos \theta}{(\varepsilon - \varepsilon_2^-) + i\Gamma/2} P_l(\cos \theta'),$$

$$l=1, \quad \Gamma = \Gamma(\varepsilon) = \frac{2}{3} \varepsilon \left( \frac{\varepsilon}{|\varepsilon_1|} \right)^{1/2}, \quad (9)$$

$$\varepsilon_2^- = \frac{\hbar^2}{m_h f^2} \frac{(f-R)}{f} \quad \text{and} \quad |f-R| \ll f.$$

Here,  $\theta$  and  $\theta'$  are the angles between  $R$  and the wave vectors of the incident and scattered waves,  $\varepsilon_2^-$  is the energy of a resonance (quasidiscrete) level, and  $\Gamma(\varepsilon)$  is the energy width of a level which, according to the general theory of resonance scattering<sup>16</sup> for a  $p$  wave ( $l=1$ ), depends on the energy of the incident particle in accordance with the law  $\Gamma(\varepsilon) \propto \varepsilon^{l+1/2}$ . The total elastic scattering cross section has its usual form for the resonance process<sup>16</sup> and its maximum value is approximately  $|\varepsilon_1|/\varepsilon_2^-$  times greater ( $\varepsilon_2^- \ll |\varepsilon_1|$ ) than the cross section for the scattering by an isolated defect  $4\pi f^2$ . All that we have said about resonance elastic scattering applies directly to the capture of excitons by pairs of oxygen vacancies. In fact, the capture of an exciton by the ground state  $\varepsilon_2^+$  involves emission of acoustic phonons and is a channel of inelastic scattering of excitons by clusters. Such resonance scattering increases considerably the density of the exciton wave function near a pair with  $R \approx f$ , and this in turn enhances greatly the probability of capture of an exciton by the ground state with the energy  $\varepsilon_2^+$ . A direct calculation of the capture cross section  $\sigma_2$  is made by the substitu-

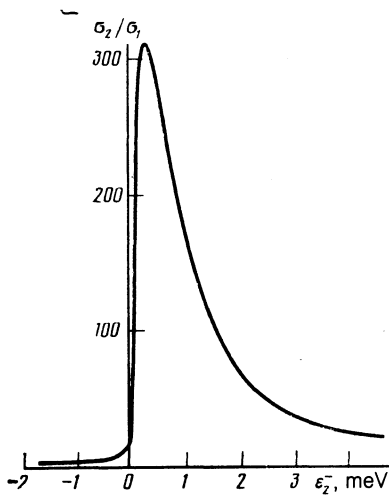


FIG. 5. Dependence of the maximum of the ratio of the exciton-capture cross sections of a pair of oxygen vacancies and of an isolated vacancy  $\sigma_2/\sigma_1$  on the energy of the excited state  $\epsilon_2^-$  of the pair in the region of a resonance.

tion of Eqs. (7) and (8) into Eq. (5), where the wave function of the final state is

$$\Psi_2 = \left\{ \frac{\kappa}{4\pi[1+\exp(-\kappa f)]} \right\}^{1/2} \left[ \frac{\exp(-\kappa|r-R/2|)}{|r-R/2|} + \frac{\exp(-\kappa|r+R/2|)}{|r+R/2|} \right], \quad \kappa = \left[ \frac{2m_h}{\hbar^2} |\epsilon_2^+| \right]^{1/2}. \quad (10)$$

After these calculations we obtain the following expression for  $\sigma_2$ :

$$\sigma_2 = \pi f^2 \frac{|\epsilon_1|}{\epsilon} \frac{\Gamma\Gamma_\Phi}{(\epsilon - \epsilon_2^-)^2 + 1/4(\Gamma + \Gamma_\Phi)^2} + \frac{w^2}{2\hbar\rho s^3} \operatorname{arctg}^2 \left[ \left( \frac{|\epsilon_2^+|^{1/2}}{2m_h s^2} \right)^{1/2} \left( \frac{|\epsilon_2^+|}{\epsilon} \right)^{1/2} \left( \frac{|\epsilon_2^+|}{|\epsilon_1|} \right)^{1/2} \right],$$

$$\Gamma_\Phi = \frac{\hbar}{\tau_\Phi} = \frac{w^2}{\pi\hbar\rho s^3 f^2} \frac{|\epsilon_2^+|^{1/2}}{|\epsilon_1|^{1/2}} \frac{\operatorname{arctg}^2 \left[ (|\epsilon_2^+|/2m_h s^2)^{1/2} \right]}{[1+\exp(-\kappa f)]}, \quad (11)$$

where  $\tau_\Phi$  is the characteristic time of a transition between the excited  $\epsilon_2^-$  and ground  $\epsilon_2^+$  states of a complex formed by an exciton and a pair of oxygen vacancies ( $R \approx f$ ), accompanied by the emission of acoustic phonons. In Eq. (10) we separated the resonance and continuous parts of the capture cross section  $\sigma_2$ . The resonance part of the cross section of the capture by a pair of oxygen vacancies is described by the Breit-Wigner formula<sup>16</sup> in which the width  $\Gamma$  of an elastic scattering resonance is given by Eq. (9). If the energy of excitons incident on a resonance cluster is  $\epsilon \sim \epsilon_2^-$ , the capture cross section  $\sigma_2$  is considerably greater than the cross section  $\sigma_1$  for the capture by an isolated vacancy, because  $(\sigma_2/\sigma_1) \sim (\epsilon_1/\epsilon_2^-)^2 \gg 1$ . Figure 5 shows the dependence of the maximum of the ratio of the capture cross sections ( $\sigma_2/\sigma_1$ ) on the position of a resonance energy level in the forbidden  $\epsilon_2^- < 0$  ( $R \gtrsim f$ ) and allowed  $\epsilon_2^- > 0$  ( $R \lesssim f$ ) exciton energy bands. This dependence in fact illustrates the extent to which the resonance influences the process of exciton capture by pairs of oxygen vacancies. It is clear that the capture is most effective at low positive values of  $\epsilon_2^-$  and that the

capture cross section of a resonance pair of oxygen vacancies can be more than two orders of magnitude greater than the capture cross section of an isolated vacancy. For this reason, out of all possible pairs of vacancy clusters with different values of radii  $R$ , only the pairs with  $R \approx f$  capture excitons readily and give rise to resonance excited states. Even the difference of  $R$  from the resonance value by an amount equal to the lattice constant alters considerably the position of the excited level  $\epsilon_2^-$  (Fig. 4) and reduces greatly the resonance part of the capture cross section  $\sigma_2^-$  (Fig. 5). This explains the small width of the experimentally observed spectral lines of the luminescence of excitons localized at pairs of oxygen vacancies. In spite of the concentration which is low compared with  $n_1$ , the giant capture cross sections of resonance pairs of oxygen vacancies ensure that they compete successfully with isolated vacancies and are manifested together with the latter in the luminescence spectra.

The resonance capture of excitons by clusters consisting of a large number of vacancies can be considered in a similar manner. Then, an increase in the possible number of resonance and similar configurations increases on increase in  $N$ , which generally speaking should result in broadening of the observed exciton luminescence lines  $E_N$  at high values of  $N$ . Therefore, the resonance mechanism of the population should appear most clearly in the pair spectrum  $E_2$ , in full agreement with the experimental results.

We shall now analyze the temperature dependence of the luminescence spectrum of localized excitons  $E_1$ - $E_5$ . We can determine the probabilities of filling the exciton states  $E_1$  and  $E_2$  by averaging the cross sections of Eqs. (6) and (11) over the distribution function of free excitons  $\chi(\epsilon)$ . It becomes obvious that the resonance mechanism is effective at temperatures  $T \ll \epsilon_2^-$  (according to our estimates, the value of  $\epsilon_2^-$  does not exceed 10 K). At high temperatures there is no preferential population of the resonance configurations, so that at such temperatures the discrete structure of the spectrum  $E_2$ - $E_5$  should disappear and the  $E_1$  lines should predominate. An increase in the excitation intensity should also result in a more uniform population of all the clusters and not just the resonance ones. This means that a considerable increase in  $J$  transforms the discrete line series  $E_2$ - $E_5$  into a band, which is on the whole in agreement with the experimental results (Fig. 3).

The resonance process of capture by pairs of oxygen vacancies accounts for the temperature dependence of the relative intensity  $I_2/I_1$  in the range  $T \lesssim 30$  K (Fig. 2). Averaging the exciton-capture cross sections  $\sigma_1$  and  $\sigma_2$  over the distribution function  $\chi(\epsilon)$  of free excitons, we obtain

$$\frac{I_2}{I_1} = \frac{n_2 \langle \sigma_2 v \rangle}{n_1 \langle \sigma_1 v \rangle} = \frac{\pi f^2}{\sigma_0} \left( \frac{|\epsilon_1|}{\epsilon_2^-} \right)^{1/2} \chi(\epsilon_2^-) \frac{\Gamma_\Phi \Gamma}{\Gamma_\Phi + \Gamma} \left( \frac{n_2}{n_1} \right), \quad (12)$$

where

$$\sigma_0 = w^2/\hbar\rho s^3.$$

The temperature dependence of Eq. (12) deduced on the assumption that the distribution function of free electrons is Maxwellian is described by the expression

$$\frac{I_2}{I_1} = \text{const} \left( \frac{|\epsilon_1|}{m_h s^2 + T} \right)^{1/2} \exp \left( -\frac{\epsilon_2^-}{m_h s^2 + T} \right). \quad (13)$$

For the purpose of estimates it is assumed in the above formula that in the energy range  $\varepsilon \lesssim m_h s^2$  the exciton distribution function is far from equilibrium. The dependence calculated from Eq. (13) is plotted in Fig. 2 and we can see the agreement with the experimental curves is good up to  $T \leq 20$  K. At higher values of  $T$  the experimental curves deviate from the  $T^{3/2}$  law because an increase in  $T$  causes the number of electrons near the resonance energy level  $\varepsilon_2^-$  to decrease. This deviation is in agreement with the general quenching of the exciton luminescence observed at  $T \sim 30$  K, but this is outside the scope of the present paper.

The unusual temperature dependence of the intensity  $I_1$  of the  $E_1$  line, manifested by a maximum at  $T = 20$  K (Fig. 2), can also be explained by resonance capture of excitons by clusters. In fact,  $I_1$  and  $I_N$  are proportional to the fraction of the captured excitons. As  $T$  increases, the capture by the  $\varepsilon_2^-$  level of pairs of oxygen vacancies and by resonance levels of other clusters becomes weaker because of the broadening of the energy spectrum of free excitons. Estimates indicate that in the temperature range  $2 < T < 20$  K the probability of resonance capture decrease, by a factor of four. Free excitons not captured by resonance clusters of oxygen vacancies are trapped by isolated vacancies and this is the reason why the luminescence line  $E_1$  is enhanced on increase in temperature.

The dependence of the luminescence spectrum on the concentration of oxygen vacancies  $n_0$  can be described in two limiting cases. At low vacancy concentrations  $n_0 < 10^{18} \text{ cm}^{-3}$  the spectra show a clear discrete structure of the luminescence lines of excitons localized at oxygen vacancy clusters. At high values of  $n_0$  we can expect migration of excitons between clusters of different sizes and configurations. In this case resonance capture processes are no longer important in the formation of the luminescence spectrum (during its lifetime an exciton can migrate to a different cluster), so that the discrete structure  $E_2-E_5$  broadens and is converted into a band. Migration of exciton excitation on gradual reduction of energy is confirmed by the experimentally detected enhancement (on increase in  $n_0$ ) of the low-frequency part of the luminescence spectrum of complexes formed from excitons and oxygen vacancy clusters (Fig. 1). The luminescence of these complexes approaches equilibrium and the maximum of the luminescence shifts to the limit of the series of lines  $\varepsilon_\infty$  (edge of the exciton-impurity energy band), the energy position of which is estimated from the experimental and theoretical results to be 25 meV.

A detailed analysis of the luminescence spectra of exciton in  $\text{SnO}_2$  given in the present study shows that the localization of excitons at oxygen vacancy clusters accounts for the existence of a series of lines converging in the low-frequency part of the spectrum. The discrete nature of this spectrum is due to the effective population of clusters with specific resonance configurations. The selective population disappears on increase in the vacancy concentration, temperature, pumping rate, which converts a discrete series of luminescence lines into a band.

It should be stressed that the experimentally observed intensities of the exciton luminescence lines localized at clusters consisting of  $N = 2, 3, 4$  oxygen vacancies differ from one another within an order of magnitude, although statistical estimates analogous to Ref. 7 would lead us to expect a considerable reduction in the concentration of clusters on increase in  $N$ . We shall assume that a significant (compared with statistical) increase in the concentration of clusters consisting of  $N$  oxygen vacancies is due to the tendency of defects to form clusters, i.e., due to the clusterization trend. Our analysis does not deal with the mechanism of clusterization of oxygen vacancies in  $\text{SnO}_2$  but considers the possibility of determination of geometric parameters and physical properties of oxygen vacancy clusters manifested in the luminescence spectra of bound excitons. The knowledge of the actual clusterization mechanism would have allowed us to calculate the relative concentrations of clusters and compare them with the data deduced by exciton spectroscopy.

Excitons localized at groups of impurities have been observed also in spectra of other semiconductor crystals. Calculations carried out by the method described above are in agreement with the experimental results on the luminescence of localized excitons in Si and CdS crystals.<sup>6,7</sup>

The authors are grateful to Yu. A. Stepanov for his help in the experiments, and to I. P. Ipatova and V. I. Perel' for discussing the results.

<sup>1</sup>Here and later the binding energy  $\varepsilon_N$  is measured from the bottom of the exciton band, i.e., from the energy of the 1S free-exciton line  $E_0$ .

<sup>1</sup>M. Gal, Phys. Rev. B **18**, 803 (1978).

<sup>2</sup>E. Molva and N. Magnea, Phys. Status Solidi B **102**, 475 (1980).

<sup>3</sup>J. A. Kash, H. Mariette, and D. J. Wolford, Phys. Rev. B **32**, 3753 (1985).

<sup>4</sup>H. Fieseler, A. Haufe, R. Schwabe, and J. Streit, J. Phys. C **18**, 3705 (1985).

<sup>5</sup>V. T. Agekyan, Pis'ma Zh. Eksp. Teor. Fiz. **29**, 475 (1979) [JETP Lett. **29**, 431 (1979)].

<sup>6</sup>P. D. Altukhov, K. N. El'tsov, and A. A. Rogachev, Pis'ma Zh. Eksp. Teor. Fiz. **31**, 30 (1980) [JETP Lett. **31**, 27 (1980)].

<sup>7</sup>O. Goede, W. Heimbrodt, and R. Müller, Phys. Status Solidi B **105**, 543 (1981).

<sup>8</sup>Yu. M. Pokotilo, V. D. Tkachev, and V. Yu. Yasvid, Fiz. Tekh. Poluprovodn. **15**, 2034 (1981) [Sov. Phys. Semicond. **15**, 1179 (1981)].

<sup>9</sup>M. Nagasawa and S. Shionoya, Phys. Lett. **22**, 409 (1966).

<sup>10</sup>V. T. Agekyan, Opt. Spektrosk. **29**, 741 (1970) [Opt. Spectrosc. (USSR) **29**, 395 (1970)].

<sup>11</sup>V. T. Agekyan, Yu. A. Stepanov, and I. P. Shiryapov, Fiz. Tekh. Poluprovodn. **6** 1931 (1972) [Sov. Phys. Semicond. **6**, 1658 (1973)].

<sup>12</sup>K. J. Button, C. G. Fonstad, and W. Dreybrodt, Phys. Rev. B **4**, 4539 (1971).

<sup>13</sup>V. T. Agekyan, Pis'ma Zh. Eksp. Teor. Fiz. **23**, 574 (1976) [JETP Lett. **23**, 526 (1976)].

<sup>14</sup>E. I. Rashba, Fiz. Tekh. Poluprovodn. **8**, 1241 (1974) [Sov. Phys. Semicond. **8**, 807 (1974)].

<sup>15</sup>Yu. N. Demkov and V. N. Ostrovskii, Method of Zero-Radius Potential in Atomic Physics (in Russian), Leningrad State University (1975), p. 240.

<sup>16</sup>L. D. Landau and E. M. Lifshitz, *Quantum Mechanics: Non-Relativistic Theory*, 3rd ed., Pergamon, Oxford (1977).

Translated by A. Tybulewicz